Chemistry of Metals and Alloys

Chem. Met. Alloys 19 (2026) 6-11
ISSN 1998-8079 (print), ISSN 1998-8087 (online)
Ivan Franko National University of Lviv
https://publications.lnu.edu.ua/chemetal

Structural and magnetocaloric properties of TmAuGe

A. SZYTUŁA[1], J. PRZEWOŹNIK[2], Ł. GONDEK[2], P. PIEKARZ[3], D. KACZOROWSKI[4]*

[1] *Jagiellonian University, Faculty of Physics, Astronomy and Applied Computer Science, M. Smoluchowski Institute of Physics, Prof. Stanisława Łojasiewicza 11, 30-348 Kraków, Poland*
[2] *Faculty of Physics and Applied Computer Science, AGH University of Krakow, Al. Mickiewicza 30, 30-059 Kraków, Poland*
[3] *Institute of Nuclear Physics, Polish Academy of Science, W.E. Radzikowskiego 152, 31-342 Kraków, Poland*
[4] *Institute of Low Temperature and Structure Research, Polish Academy of Sciences, Okólna 2, 50-422 Wrocław, Poland*
* *Corresponding author. E-mail: d.kaczorowski@intibs.pl*

Received April 20, 2026; accepted June 25, 2026, available online September 8, 2026
https://doi.org/10.30970/cma19.0458

The hexagonal ferromagnet TmAuGe with T_C = 4.1 K was studied in a broad range of temperatures by means of X-ray diffraction (T = 3.8-300 K) and heat capacity (T = 1.8-295 K) measurements. The results revealed an unusual behavior of the lattice parameter c showing a distinct anomaly at T_C and a broad minimum near 25 K. The specific heat exhibits a clear Schottky contribution near 70 K. The magnetocaloric effect at T_C yields a magnetic entropy change of 2.3 J/(mol K) and an adiabatic temperature change of 2.75 K in a magnetic field of 0.6 T. The experimental characterization of TmAuGe was accompanied by *ab-initio* calculations of the lattice dynamics.

X-ray diffraction / Temperature evolution of lattice parameters / Heat capacity / Schottky anomaly / CEF levels / Magnetocaloric effect

1. Introduction

As established *via* X-ray and neutron diffraction experiments [1-4], most of the ternary *RE*AuGe intermetallics (*RE* = Sc, Y, La-Nd, Sm, Gd-Lu) crystallize with a hexagonal crystal structure of the LiGaGe type [5,6], which harbors an ordered arrangement of the Au and Ge atoms. Magnetic and neutron diffraction studies indicated that LaAuGe and LuAuGe are Pauli paramagnets, CeAuGe is a ferromagnet (FM), while the materials based on *RE* = Pr, Nd, Sm, Eu, Tb-Er order antiferromagnetically (AFM) at low temperatures [1,4]. The compound TmAuGe was reported to exhibit long-range FM below 4.1 K [7], and a recent investigation of single-crystalline samples revealed that the Tm magnetic moment is parallel to the hexagonal *c*-axis [8]. In contrast to the other *RE*AuGe phases, which were described as fairly good metals [9,10], TmAuGe shows a semimetallic character of the electrical conductivity [7].

Here, we report on low-temperature variations of the crystal lattice parameters and the specific heat of TmAuGe. The experimental results have been interpreted in terms of *ab-initio* calculations of the phononic characteristics, while the specific heat data has allowed developing a crystalline electric field (CEF) model that accounts for the observed Schottky contribution. In addition, the magnetocaloric properties of TmAuGe near the Curie temperature have been determined. Our study aimed to contribute to the renewed interest in the *RE*AuGe series [8-10], established most recently as a new class of Kramers nodal line (KNL) semimetals with anomalous magnetotransport behavior [11].

2. Experimental

A polycrystalline sample of TmAuGe was prepared by arc-melting stoichiometric amounts of high-purity elements (Tm – 3N, Au and Ge – 4N). The synthesis was performed on a water-cooled copper hearth in a purified argon atmosphere using Ti as a getter. The button was re-melted several times to promote homogeneity. Subsequently, the product was annealed at 773 K for 1 week.

X-ray powder diffraction (XRD) studies were performed in the temperature range 3.8-300 K using a Siemens D5000 diffractometer with CuK_α radiation,

equipped with an Oxford Instruments liquid helium cryostat. The cryostat was adjusted against temperature displacements using a high-purity (6N) tungsten standard, which provided a temperature stabilization better than 0.06 K. The XRD data were analyzed employing the Rietveld-type software FullProf [12].

Specific heat measurements were carried out in the temperature interval 1.8-295 K using the relaxation method implemented in a Quantum Design PPMS-9 platform. The specific heat data were collected also between 1.8 K and 15 K in an external magnetic field up to 0.6 T.

3. Results

3.1. Structural properties

The XRD pattern of TmAuGe collected at T = 300 K was easily indexed within a hexagonal LaGaGe-type structure (space group $P6_3mc$, No. 186) with the lattice parameters: a = 4.3908(5) Å and c = 7.1659(8) Å. The final Bragg R factor of 5.76% and N_{scor} = 2.81 indicate good quality of the performed refinement. The unit cell of TmAuGe is shown in Fig. 1. The constituent atoms are located at the following sites: Tm at Wyckoff position 2*a* (0,0,0), Au at 2*b* (⅓,⅔,0.2114(2)), and Ge at 2*b* (⅓,⅔,0.7961(3)), and form a three-dimensional network.

The temperature dependence of the lattice parameters is displayed in Fig. 2. Above 30 K, both parameters increase with increasing temperature, yet the unit cell expansion is anisotropic. The linear thermal expansion along the *a*-axis equals 1.6 10^{-5} K^{-1} and that along the *c*-axis is 0.6 10^{-5} K^{-1}. At low temperatures, there occurs no anomaly in the *T*-dependence of the *a*-parameter, except for a marked change in its slope near 25 K. In the same region, the *c*-parameter shows an anomalous upturn, followed by a step-like drop at the onset of the FM state at T_C = 4.1 K (see the inset to Fig. 2).

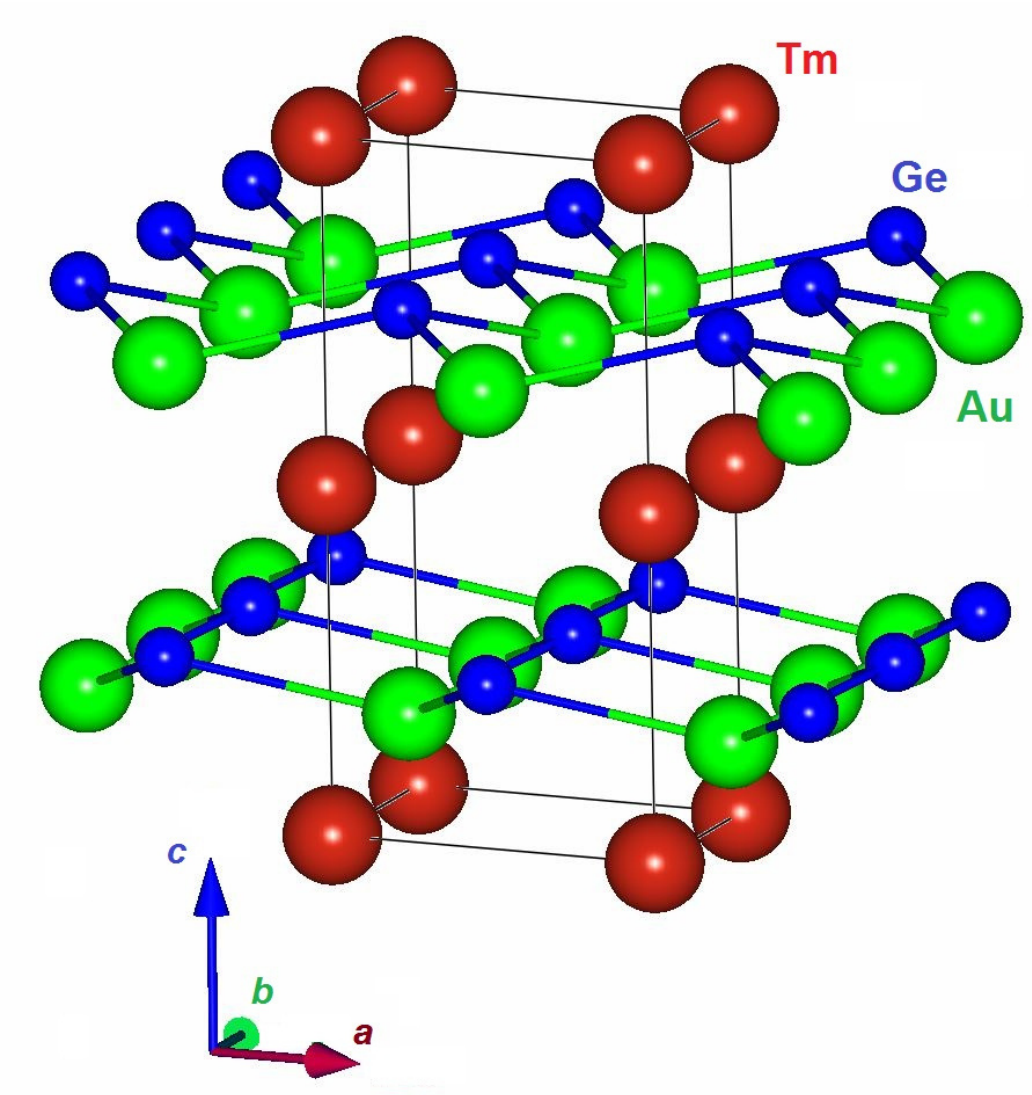

Fig. 1 The crystal structure of TmAuGe. The quasi two-dimensional [Au Ge] networks are emphasized.

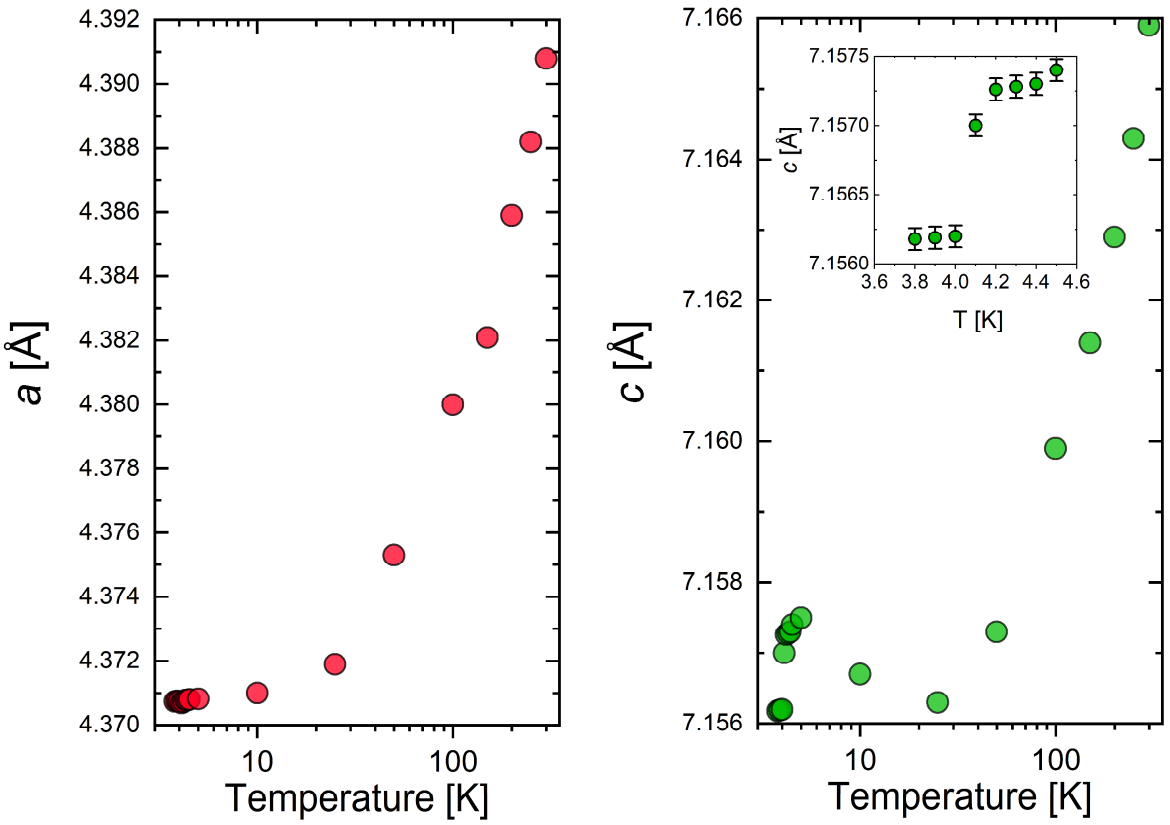

Fig. 2 Temperature dependencies of the lattice parameters of TmAuGe. The inset shows the variation of the lattice parameter *c* near the Curie temperature T_C.

3.2. Heat capacity

The temperature dependence of the specific heat of TmAuGe is presented in Fig. 3. It exhibits a typical sigmoid-like shape and a sharp lambda-shaped peak at T_C = 4.1 K. The jump in $C_p(T)$ at the onset of the FM state amounts to about 10 J/(mol K), which is fairly close to the value of 12.47 J/(mol K) predicted for ferromagnets within the molecular field approximation (MFA).

In order to extract the magnetic contribution $C_{Magn}(T)$ to the specific heat of TmAuGe, the $C_p(T)$ variation was measured for the non-magnetic isostructural compound LaAuGe. The collected data were rescaled according to the different atomic masses of La and Tm, and the result is shown in Fig. 4 (note the dashed blue line). Clearly, the obtained curve cannot be used as an estimate of the phonon contribution to the specific heat of TmAuGe, as it surpasses the measured data in the region 12-30 K and above 240 K. This finding hints at substantially different phononic properties of the two investigated compounds.

Another attempt to estimate $C_{Magn}(T)$ was *via* calculation of the lattice contribution in TmAuGe from first principles. In the first step, the crystal structure of the compound was optimized within the generalized gradient approximation (GGA) using the VASP program [13]. The calculations were carried out for six atoms in the 1 × 1 × 1 supercell with periodic boundary conditions. The experimental lattice parameters and atomic positions were taken as the input data, and the valence electron configurations were assumed to be Ge $4s^24p^2$, Au $5d^{10}6s^1$ and Tm $4f^{12}$. Subsequently, the phonon frequencies were calculated by means of the direct method implemented in the PHONON program [14]. In this approach, the Hellmann-Feynman forces are computed by displacing atoms from their equilibrium positions. From the atomic displacements and forces, the force constant elements were obtained by the singular value decomposition method. Having the force constants and dynamical matrices, phonon frequencies were calculated for each of the *k*-points. The so-calculated phonon dispersion curves are presented in Fig. 4. It is worth noting that the optical modes show no degeneracy. Remarkably, there are some soft optical modes that cross the acoustic ones. Finally, the lattice heat capacity of TmAuGe was obtained with the harmonic approximation, using a standard thermodynamic approach, and the derived curve is shown by the red solid line in Fig. 3. Upon subtracting this data from the experimental

specific heat of TmAuGe, $C_{Magn}(T)$ and the corresponding magnetic entropy were estimated (see the inset to Fig. 3). As can be inferred from this figure, the magnetic entropy released at T_C amounts to 4.41 J/(mole K), which is about 77% of Rln2, *i.e.*, the value expected for a doublet CEF ground state. Above T_C, $S_{Magn}(T)$ remains nearly constant up to *ca.* 25 K, and then asymptotically increases towards Rln13, expected for the full Tm^{3+} multiplet, however the latter value is not achieved even at room temperature, hence signaling fairly large total CEF splitting.

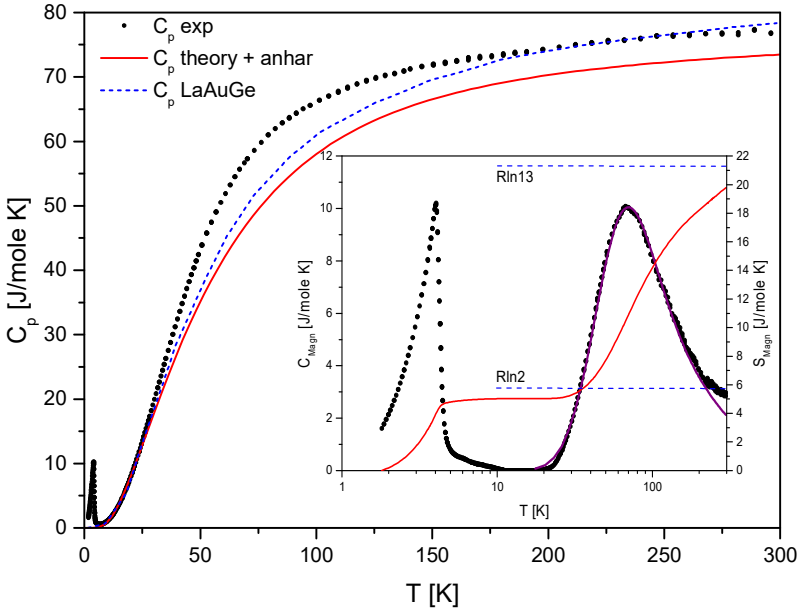

Fig. 3 Temperature variation of the specific heat of TmAuGe (black dots). The dashed blue curve represents the specific heat of the non-magnetic isostructural counterpart LuAgGe (corrected for the difference in the atomic masses of Lu and Tm). The red solid curve is the lattice contribution to the specific heat of TmAuGe calculated as described in the text. The inset displays the estimated magnetic contribution to the specific heat of TmAuGe (circles) and the magnetic entropy (red line). The purple curve represents the Schottky contribution derived as described in the text.

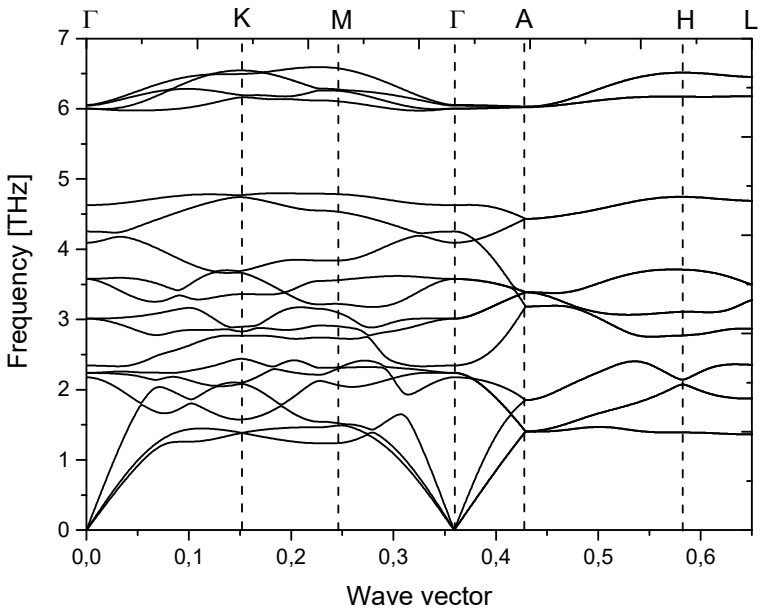

Fig. 4 Phonon dispersion relation along the high symmetry directions within the Brillouin zone. The special points are Γ (0,0,0), K (½,½,0), M (½,0,0), A (0,0,½), H (½,½,½), and L (½,0,½).

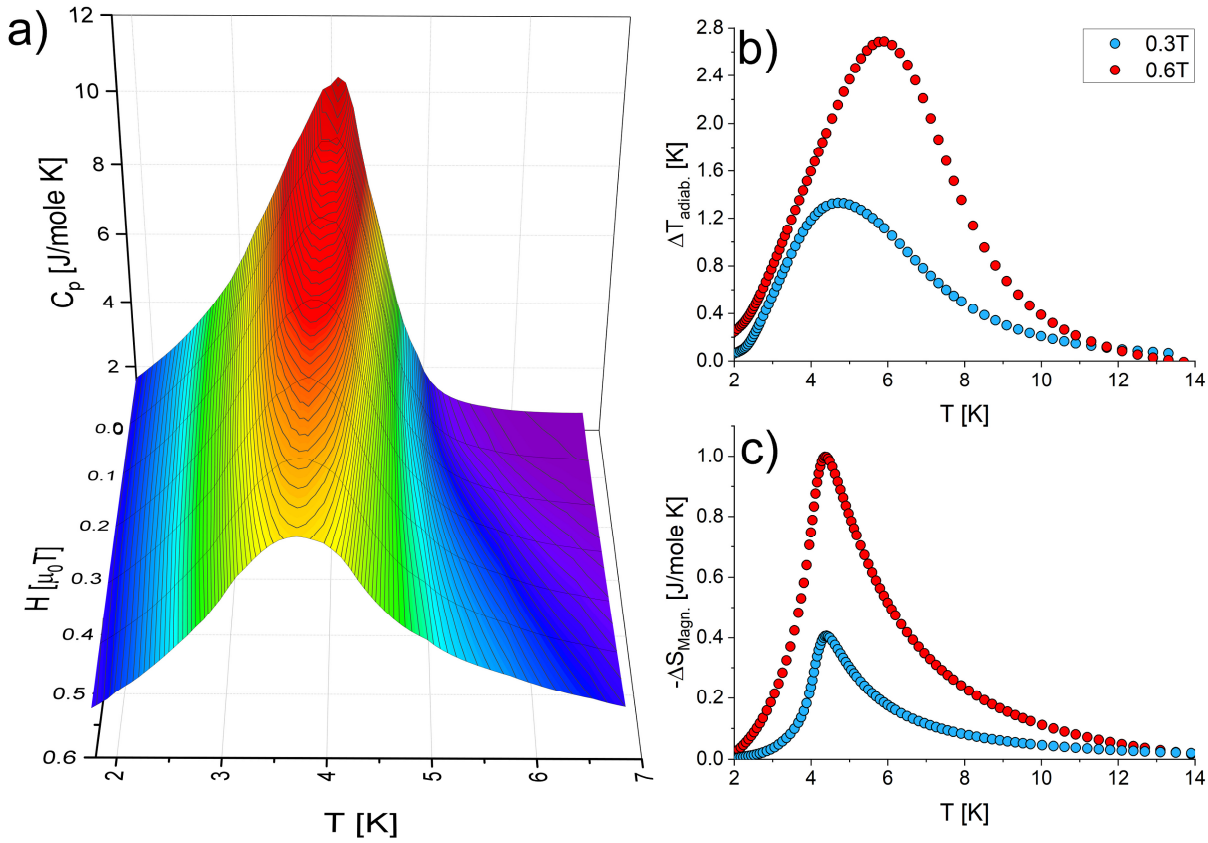

Fig. 5 (a) Temperature dependencies of the specific heat of TmAuGe measured near the FM phase transition in various external magnetic fields. (b) and (c) Low-temperature variations of the adiabatic temperature change and the magnetic entropy change in TmAuGe, respectively, determined in magnetic fields of 0.3 T (blue symbols) and 0.6 T (red symbols).

In the CEF potential of relatively low local symmetry (C_{3v}), the ground multiplet of the Tm^{3+} ions in the crystal lattice of TmAuGe splits into 4 doublets and 5 singlets. As shown in the inset to Fig. 3, the Schottky contribution to the specific heat of ThAuGe can be well approximated (note the purple line) within the following CEF model: 0 K (doublet), 131 K (singlet), 172 K (doublet), 195 K (singlet), 226 K (doublet), 256 K (doublet), 534 K (singlet), 602 K (singlet), 622 K (singlet). Despite the satisfactory description of the experimental data, it should be noted that the positions of the CEF levels lying above 300 K were obtained with significant uncertainties. Furthermore, it is also possible that the derived energy scheme is not a unique scenario of the actual CEF splitting in TmAuGe.

3.3. Magnetocaloric effect

Fig. 5a shows the temperature dependencies of the specific heat of TmAuGe in the vicinity of the Curie temperature in different external magnetic fields up to 0.6 T. With increasing field the lambda-shaped peak in $C_p(T)$ decreases and broadens. Based on these data the magnetocaloric effect (MCE) was calculated. The magnetic entropy change ΔS_{Magn} was derived using an integral version of the Maxwell thermodynamics. The maximum value obtained near T_C equals 0.4 J/(mol K) in a field of 0.3 T and 1.0 J/(mol K) in a field of 0.6 T (see Fig. 5c). These values are similar to those reported for EuAuGe (1.7 J/(kg K) in 1 T [15]) or other Tm-intermetallics (see the data collected in Table 2 in Zheng *et al.* [16]). In turn, the adiabatic temperature change ΔT_{adiab}, defined as $\Delta T_{adiab}(\Delta H, T) = [T(S_{Magn})_{H1} - T(S_{Magn})_{H0}]S$, where $\Delta H = H_1 - H_0$, attains a magnitude of 2.75 K near 7 K (see Fig. 5b). This value is similar to those reported for intermetallic magnetocaloric materials [17].

4. Conclusions

The hexagonal LiGaGe-type crystal structure of TmAuGe, previously determined at room temperature [7,8], was found to persist down to at least 3.8 K. With decreasing temperature, the lattice parameter *c* initially decreases regularly, then shows an anomalous increase below 25 K followed by a step-like drop at the FM phase transition (T_C = 4.1 K [7]). In contrast, the lattice parameter *a* decreases systematically, showing only a change in the slope of the $a(T)$ curve near 25 K. The origin of this singularity remains unclear. It is unlikely to stem from CEF interactions,

as the $C_p(T)$ data indicate that the first excited CEF level is situated well above the ground doublet, at approximately 131 K. On the other hand, according to Schnelle *et al.* [3], the non-magnetic compounds *RE*AuGe (*RE* = Sc, Y, La, Lu) exhibit unusual phononic characteristics in the temperature range 10-20 K. By analogy to those phases, one can assume that a similar effect occurs also in TmAuGe, and the features near 25 K are driven by some abnormal enhancement of the force constants.

The CEF model developed for TmAuGe based on the specific heat data accounts for the splitting of the $^3H_6$ multiplet of the Tm^{3+} ion in C_{3v} symmetry into four doublets and five singlets. The estimated energy positions of the CEF levels are similar to those derived before by Kurumaji *et al*. [8]. In particular, the separation of the ground doublet and the first excited singlet is almost the same.

Near T_C, TmAuGe exhibits enhanced magnetocaloric properties. The maximum magnetic entropy change reaches 2.3 J/(mol K) in a field change of 0.6 T, while the adiabatic temperature change is 2.7 K. These parameters make the compound a promising candidate for magnetic refrigeration.

Acknowledgements

This research was supported in part by the Excellence Initiative – Research University Programme at the Jagiellonian University in Kraków. A. Szytuła gratefully acknowledges Dr Stanisław Baran (Jagiellonian University, Faculty of Physics, Astronomy and Applied Computer Science, M. Smoluchowski Institute of Physics, Kraków, Poland) for his help and discussion on the final version of the work.

References

[1] B.J. Gibson, Thesis, Loughorough University, 1998.
[2] R. Pöttgen, H. Borrmann, C. Felser, O. Jepsen, R. Henn, R.K. Kremer, A. Simon, *J. Alloys Compd.* 235 (1996) 170. https://doi.org/10.1016/0925-8388(95)02069-1
[3] W. Schnelle, R. Pöttgen, R.K. Kremer, E. Gmelin, O. Jepsen, *J. Phys.: Condens Matter* 9 (1997) 1435. https://doi.org/10.1088/0953-8984/9/7/009
[4] S. Baran, M. Hofmann, B. Penc, M. Ślaski, A. Szytuła, A. Zygmunt, *Physica B* 276-278 (2000) 656. https://doi.org/10.1016/S0921-4526(99)01741-X
[5] W. Bockelmann, H. Jacobs, H.-U. Schuster, *Z. Naturforsch B* 25 (1970) 1305. https://doi.org/10.1515/znb-1970-1120
[6] W. Bockelmann, H.-U. Schuster, *Z. Anorg. Allg. Chem.* 410 (1974) 233. https://doi.org/10.1002/zaac.19744100303
[7] D. Kaczorowski, A. Szytuła, *J. Alloys Compd.* 614 (2014) 186. https://doi.org/10.1016/j.jallcom.2014.06.047
[8] T. Kurumaji, M. Gen, S. Kitou, K. Ikeuchi, M. Nakamura, A. Ikeda, T. Arima, *J. Alloys Compd.* 947 (2023) 169475. https://doi.org/10.1016/j.jallcom.2023.169475
[9] T. Kurumaji, M. Gen, S. Kiton, T. Arima, *Phys. Rev. B* 110 (2024) 064409. https://doi.org/10.1103/PhysRevB.110.064409
[10] D. Ram, J. Singh, M.K. Hooda, K. Singh, V. Kanchana, D. Kaczorowski, Z. Hossain, *Phys. Rev. B* 108 (2023) 235107. https://doi.org/10.1103/PhysRevB.108.235107
[11] T. Kurumaji, J. I. Facio, N. Mitsuishi, S. Imajo, M. Gen, M. Kimata, L. Ye, D. Graf, M. Sakano, M. Kitamura, K. Yamagami, K. Ishizaka, K. Kindo, T. Arima, *Adv. Sci.* 12 (2025) 2501669. https://doi.org/10.1002/advs.202501669
[12] J. Rodriguez-Carvajal, *FullProf,* Version 2.8, July 2004, ILL.
[13] G. Kresse, J. Furthmüller, *Comput. Mater. Sci.* 6 (1996) 15. https://doi.org/10.1016/0927-0256(96)00008-0
[14] K. Parliński, Z.Q. Li, Y. Kawazoe, *Phys. Rev. Lett.* 78 (1997) 4063. https://doi.org/10.1103/PhysRevLett.78.4063
[15] Y. Zhang, G. Wilde, *J. Supercond. Novel Magn.* 29 (2016) 2159. https://doi.org/10.1007/s10948-016-3519-x
[16] S. Zheng, N. Sun, Q. Zhang, K. Zhao, Q. Dai, X. Zhao, J. Cheng, J. Hung, *Cryogenics* 147 (2025) 104056. https://doi.org/10.1016/j.cryogenics.2025.104056
[17] L.M. Moreno-Ramirez, D.P. Rojas, J.I. Espeso, J. Rodriguez-Fernandez, V. Franco, *J. Rare Earths* 44 (2026) 249. https://doi.org/10.1016/j.jre.2025.03.010

Authors and ORCID IDs:
A. SZYTUŁA: 0000-0002-5196-8594
J. PRZEWOŹNIK: 0000-0002-2313-7611
Ł. GONDEK: 0000-0002-4149-7944
P. PIEKARZ: 0000-0001-6339-2986
D. KACZOROWSKI: 0000-0002-8513-7422